An Analysis of Valve Train Behavior Considering Stiffness Effects

Dong-Joon Chun*
Department of Automotive Engineering, Byuksung College
Jin-Kab Lee
LG Electronics Inc.

To maintain the specific volumetric efficiency of a heavy-duty diesel engine, an understanding of the behavior of each part of the valve train system is very important. The stiffness of the valve train system has a strong influence on the behavior of the valve train than valve clearance, heat-resistance, or the durability of parts. In this study, a geometrical cam design profile using a finite element model of the valve train system is suggested. The results of the valve behavior according to the change in stiffness is analyzed for further tuning of the valve train system.

Key Words : Diesel Engine, Valve Train System, OHC, Finite Element Method, Stiffness

Nomenclature

C : Valve clearance
C_n : Stiffness coefficient of bracket
C : Stiffness coefficient of bracket bolt
D : Deformation
D_C : Deformation of cam shaft
D_M : Deformation of cylinder head
D_P : Deformation of push-rod
D_S : Deformation of rocker shaft and bracket
D_R : Deformation of rocker arm
D_1 : Flexural deflection of rocker shaft
D_2 : Flexural deflection of bracket
D_3 : Elongation of bracket
e : Eccentricity
E : Modulus of elasticity of rockerarm material
F : Force at rockerarm valve end
F_0 : Initial mounting force of valve spring
F_G : Gas force acting on valve
h_R : Ramp height
J_m : Mean flexural moment of inertia of the rockerarm cross section
k_0 : Stiffness of valve train
k_1 : Stiffness of valve spring
m_1 : Valve effective mass
m_2 : Cam effective mass
M : Moment
N_c : Cam design speed
R_m : Mean rocker ratio
R_i : Instantaneous rocker ratio
x_0 : Actual tappet lift
y_0 : Equivalent tappet lift

* Corresponding Author,
E-mail : djchun@mail. byuksung-c. ac. kr
TEL : +82-658-540-2403
Department of Automotive Engineering, Byuksung College, 51-25, Gongduck-ri, Gongduck-myun, Kimje-shi Chonbuk 576-711, Korea (Manuscript **Received** March 24, 1999; **Revised** December 13, 1999)

1. Introduction

To maintain the specific volumetric efficiency of engines, understanding the normal behavior of a valve train system is important. The stiffness of a valve train has more significant influence on the operation of an engine than static valve clearance, durability, or heat resistance. Especially for OHC type valve trains of a turbocharged diesel engine, the dynamic behavior of its valve train is influenced by engine vibration, and thus each part of the valve train system has to be tuned for optimum conditions (Yan, et al., 1996; Chan, et al., 1987; Kim, et al., 1990). The predictive analysis of valve trains mainly relies on valve acceleration data, because it provides information on the dynamic characteristics of the valve train system (Sakai and Kosaki; 1976). The mass property data that is associated with the tuning of the valve train can be measured, but the stiffness data associated with tuning cannot be directly measured; it can instead be calculated using the natural frequency and deformation of the rocker arm, cam shaft, rockcker arm shaft, mounting brackets, etc. Furthermore, it has many dependent coefficients which are difficult to analyze.

Some of the previous studies on the optimization of the dynamic behavior of valve trains include the optimized design of cam profile (Hrones, 1948; Shooter, et al., 1994; Dudley, 1948). The cam and rocker arm are interrelated with the operating mechanism. The behavior of the contact area is important, especially for the cam profile design which affects the acceleration of the valve. If the rocker arm always contacts along the base circle by actuating the cam, the valve will not be closed. To prevent the above phenomena, maintaining a valve clearance is necessary. This clearance in turn, affects the valve acceleration. Furthermore, wide clearance causes noise and vibration, while narrow clearance causes valve overheating and leakage of compressed gas between the valve and valve seat. The transition of the cam profile to the base circle is formed by the ramps. The most frequently used ramp types are the inflected type ramp, constant jerk type ramp and constant velocity type ramp. The inflected type ramp have the disadvantages of flexibility, clearance and tolerance. The inflected type ramp often has a problem with noise and vibration, because the actual cam profile is different from the calculated one. In the case of the constant jerk type ramp, dynamic force is transmitted to the valve train before the opening of the valve. That causes early opening of the valve even in the case of low acceleration, and furthermore it cannot be adopted in the closing phase of the valve, in which the valve should move at low velocity during the upper ramp period. In contrast to other types of ramps, the constant velocity type ramp is widely adopted. It is actuated with the same velocity regardless of clearance and flexibility, and cam lift can be changed easily without changing the operating point, which makes it easy to design the cam profile. But so far this kind of ramp design includes only valve lift curve and excludes stiffness, which affects the dynamic characteristics of the valve mechanism.

Other methods like optimization of cam profiles, which can compensate for error in the case of off-speed operation, has difficulty in formulation of the cam and rocker arm (Matter and Tesar, 1978). The results of the numerical method are also different from actual valve train behavior (Chen, 1973; Mercer and Holowenki, 1958; Seiditz 1990).

The dynamic characteristics of valve trains are important when designing an OHC type valve which has relatively higher flexibility (Kwakernaak and Smit, 1968; Barkan, 1958; Roggenbuck, 1953). In this study the finite element method was adopted to find out the dynamic behavior of the valve train. The deformation of the cam shaft, rocker arm, rocker shaft, mounting bracket, etc. was used to analyze the stiffness of the system. The whole valve train model with simple beam and mass elements was analyzed to figure out the dynamic characteristics, and the stiffness distribution of each part was represented.

2. Valve Train Analysis Model

2.1 Valve train equivalent system

The center-pivot type OHC valve train is analyzed in this study, and the equivalent valve train system can be modelled to design a cam profile as shown in Fig. 1. The valve end effective mass m_1 includes the equivalent mass of the intake valve, exhaust valve, valve spring, retainer, and rocker

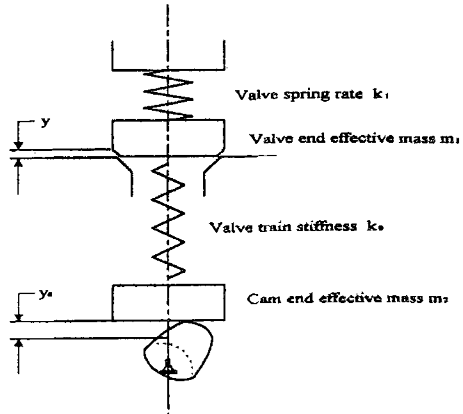

Fig. 1 Valve train equivalent system

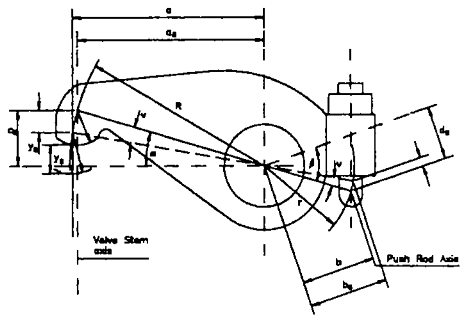

Fig. 2 Geometry of center-pivot type rocker arm

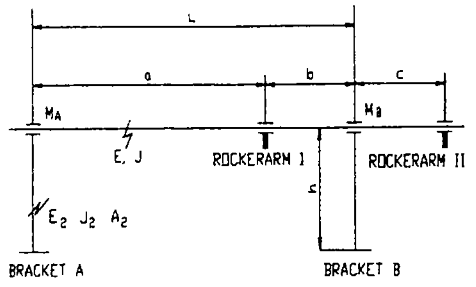

Fig. 3 A simple elastic model for the locker shaft

arm. The cam end effective mass m_2 includes the equivalent mass of the pushrod and tappet. The two masses are connected by a spring representing the valve train stiffness and held in contact with this spring by the valve spring.

Practically designed rocker arms yield a variable rocker ratio over the lift period which requires consideration in the cam design. The evaluation of this variable rocker ratio is based on the rocker arm geometry in Fig. 2. The dimensions a_0, b_0, c_0, d_0, α, β are referred to the closed valve. The polydyne cam computations yield an equivalent tappet lift y_0 which is referred to the valve. Considering the geometrical conditions, the actual tappet lift x_0 is obtained from the relation

$$x_0 = r[\sin\beta - \sin(\beta-\gamma)] \tag{1}$$

The angular movement γ of the rocker arm is obtained from the relation for the equivalent tappet lift y_0:

$$y_0 = R[\sin\alpha - \sin(\alpha-\gamma)] \tag{2}$$

$$\gamma = \alpha - \text{arc}\ \sin(\sin\alpha - \frac{y_0}{R}) \tag{3}$$

The mean rocker ratio R_m is obtained as Eq. (4) from Eq. (1) and Eq. (2), and furthermore the instantaneous rocker ratio is as given in Eq. (5):

$$R_m = \frac{y_0}{x_0} = \frac{R[\sin\alpha - \sin(\alpha-\gamma)]}{r[\sin\beta - \sin(\beta-\gamma)]} \tag{4}$$

$$R_i = \frac{a}{b} = \frac{R\cos(\alpha-\gamma)}{r\cos(\beta-\gamma)} \tag{5}$$

2.2 Valve train stiffness

The valve train stiffness is determined by the ratio of a certain force applied to the rocker arm valve end divided by the resulting total deflection occurring at the rocker arm valve end, i.e.,

$$k_0 = \frac{F}{D} \tag{6}$$

The total valve train deflection occurring at the rocker arm valve end due to the applied force is the sum of the evaluated deflections of the individual valve train components plus an estimated deflection of miscellaneous parts:

$$D = D_R + D_S + D_P + D_C + D_M \tag{7}$$

The deflection of the rocker arm can be calculated from the following simplified formula and furthermore can be replaced as a moment of inertia from experience:

$$D_R = \frac{FL^3}{3EJ_m}\frac{R_i^2}{(R_i+1)^2} \tag{8}$$

The deflection of the rocker arm shaft and brackets can be calculated as a sum of deflections occuring at the rocker arm valve end due to a force applied in this position. The evaluation of the shaft deflections is based on the formulas for a straight bar which is elastically restrained by the supports as shown in Fig. 3. The flexural deflection of the shaft at position I can be calculated as follows:

$$D_\text{I} = (R_i+1)^2\left[\frac{Fa^2b^2}{3EJL} - \frac{M_A}{6EJ}(Lb - \frac{b^3}{L}) - \frac{M_B}{6EJ}(La - \frac{a^3}{L})\right] \tag{9}$$

where M_A and M_B represent the moment positions A and B, respectively. The flexural deflection and elongation of the brackets at position II can be calculated as follows:

$$D_2+D_3=(R_i+1)^2\left[\frac{FHe^2}{E_2J_3}+\frac{F}{C_S+C_B}\right]\frac{a^2+b^2}{L^2} \tag{10}$$

where e is the eccentricity of the rocker shaft axis, H is the distance from bracket bottom to rocker shaft center, and C_S and C_B are the longitudinal stiffness of the bracket and bolt, respectively.

These formulas include certain simplifications, in particular for the more complex parts. The described calculation procedure for the valve train stiffness is to be regarded more or less as an estimation rather than an exact evaluation but yields sufficiently accurate results for cam design purposes.

2.3 Cam design

For the analysis of structural deformation, the polydyne cam profile was used. The polynomial cam profile assumes that the valve train is a rigid body, but the polydyne cam profile considers elastic deformation of the valve train parts which was affected by the dynamic effects of the cam movement. For the polydyne cam design, the following polynomial is used for the evaluation of the valve lift curve:

$$y=L(1+c_2x^2+c_4x^4+c_px^p+c_qx^q+c_rx^r+c_sx^s) \tag{11}$$

where L is a maximum lift above ramps at $x=0$, $c's$ are coefficients calculated from the boundary conditions, x is the cam angle measured from the point with maximum lift to half the main event length.

The equivalent tappet lift is determined, which provides the assessed valve lift:

$$y_0=h_R+\sigma y+\delta y'' \tag{12}$$

where

$$\sigma=\frac{k_o+k_1}{k_0} \tag{13a}$$

$$\delta=\frac{36\ N_C^2m_1}{1000k_0} \tag{13b}$$

Here h_R is the ramp height, k_1 is the stiffness of the valve spring, and N_C is the cam design speed.

For the standard ramp, the equivalent tappet lift and its derivations as well as the cam angles at the ends of the two sections are obtained from the following formulas. Eqs. (14a) to (14d) are for the constant velocity region, while Eqs. from (15a) to (15d) are for the constant acceleration region:

$$y_R=h_R-R_R(\Phi_1-a) \tag{14a}$$

$$y_R'=-R_R \tag{14b}$$

$$y_R''=0 \tag{14c}$$

$$\Phi_1=a+\frac{0.75h_R}{R_R} \tag{14d}$$

$$y_R=\frac{R_R^2}{h_R}(\Phi_2-\Phi)^2 \tag{15a}$$

$$y_R'=\frac{2R_R^2}{h_R}(\Phi_2-\Phi) \tag{15b}$$

$$y_R''=\frac{2R_R^2}{h_R} \tag{15c}$$

$$\Phi_2=\Phi_1+\frac{h_R}{2R_R} \tag{15d}$$

Table 1 summarizes the boundary conditions for determining the polynomial curve of the valve lift. Substituting these boundary conditions for the polynomial equation yields five linear equations for determining the coefficients c_2, c_p, c_q, c_r, c_s. c_4 is a free coefficient by which the shape of the acceleration curve in its negative branch may be varied for optimization of the cam profile, e. g. adaptation of deceleration to the spring characteristic, achieving uniform contact stress, etc.

$$c_2+c_p+c_q+c_r+c_s=-1-c_4 \tag{16a}$$

$$2c_2+pc_p+qc_q+rc_r+sc_s=-4c_4 \tag{16b}$$

$$2c_2+p(p-1)c_p+q(q-2)c_q+r(r-1)c_r+s(s-1)c_s=-12c_4 \tag{16c}$$

$$p(p-1)(p-2)c_p+q(q-1)(q-2)c_q+r(r-1)(r-2)c_r+s(s-1)(s-2)c_s$$

Table 1 Summary of boundary conditions

Boundary	Value
cam end	$y(1)=0$ $y'(1)=0$ $y''(1)=0$ $y^{IV}(1)=0$
	$y_0'''(1)=0$
ramp to cam junction	$y'''(1)=-R_R/\delta$
	$y_0'(1)=-R_R$

$$= -(a^3 R_R \delta L) - 24c_4 \qquad (16d)$$

$$p(p-1)(p-2)(p-3)c_p + q(q-1)(q-2)(q-3)c_q + r(r-1)(r-2)(r-3)c_r + s(s-1)(s-2)(s-3)c_s = -24c_4 \qquad (16e)$$

For a valve train with a variable rocker ratio over the lift period, the actual tappet lift and its first and second derivations are obtained from the following relations:

$$z_0 = r[\sin\beta - \sin(\beta-\gamma)] = r[\sin\beta - \sin\{\beta - \alpha + \arcsin(\sin\alpha - \frac{y_0}{R})\}] \qquad (17a)$$

$$z'_0 = y'_0 \frac{r}{R}[\cos(\beta-\alpha) - \frac{\sin(\beta-\alpha)(\sin\alpha - \frac{y_0}{R})}{\sqrt{1-(\sin\alpha-\frac{y_0}{R})^2}}] \qquad (17b)$$

$$z''_0 = \frac{r}{R}[y''_0\{\cos(\beta-\alpha) - \frac{\sin(\beta-\alpha)(\sin\alpha-\frac{y_0}{R})}{\sqrt{1-(\sin\alpha-\frac{y_0}{R})^2}} + \frac{(y'_0)^2}{R}\frac{\sin(\beta-\alpha)}{\sqrt{\left\{1-(\sin\alpha-\frac{y_0}{R})^2\right\}^3}}] \qquad (17c)$$

To ensure that both opening and closing of the valves actually occurs on the ramps, the ramp heights must equal or exceed the following equivalent values:

$$h_R \geq C + \frac{F_0}{k_0}$$

; for intake opening side (18a)

$$h_R \geq C + \frac{F_0}{k_0} + \frac{F_G}{k_0}$$

; for exhaust opening side (18b)

$$h_R \geq C + \frac{F_0}{k_0} + \Delta h_R$$

; for intake and exhaust closing side (18c)

The above ramp equations are provided to control impact at the valve opening side and seating velocity at the closing side of the cam.

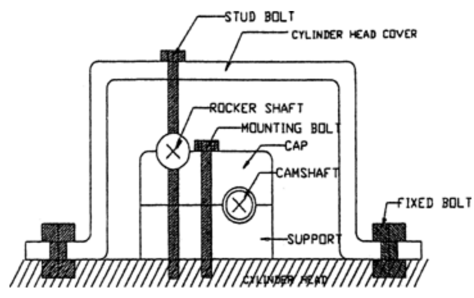

Fig. 4 Simple elastic model of rocker shaft

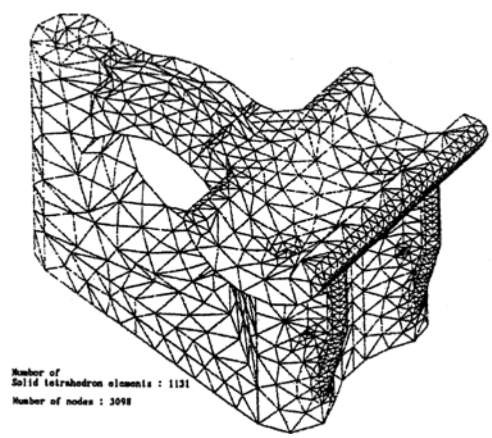

Fig. 5 Finite element model of cap and support bracket

3. Finite Element Model

The Finite element technique was used to deternine the dynamic characteristics of the valve mechanism, especially its stiffness. Figure 4 represents the cross section of the upper valve train parts of the cylinder head which was modelled with mass and beam elements. Figure 5 represents the finite element model using solid tetrahedron elements of the bracket consisting of the cap and support. A three dimensional modeller, the parts model and assembler modeller of the I-DEAS MASTER SERIES, and NASTRAN was used.

The stiffness of the bracket can be obtained by either applying a unit deformation to the finite element model or applying an actual force to model. Figure 6 represents the boundary and loading conditions of the finite element model. The radial directional pressure according to the

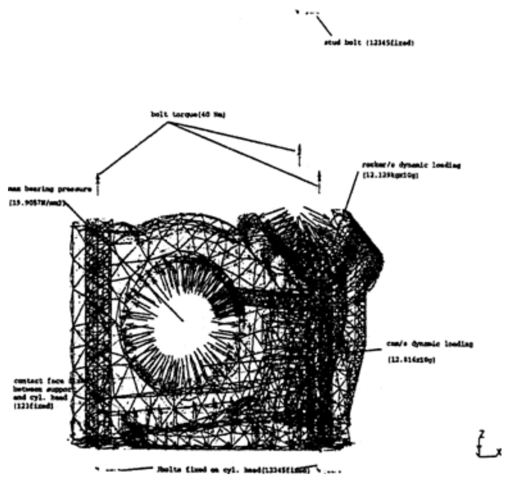

Fig. 6 Boundary and loading condition of finite element model

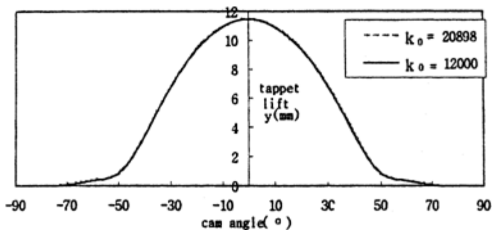

Fig. 7 Equivalent tapper life (intake)

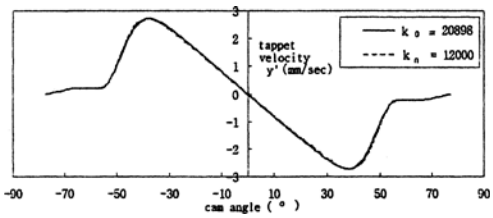

Fig. 8 Equivalent tappet velocity (intake)

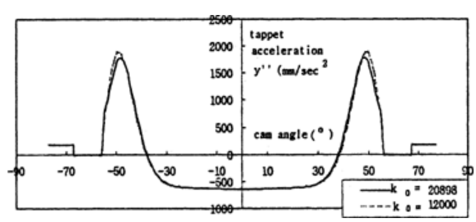

Fig. 9 Equivalent tappet acceleration (intake)

interaction between the inner bearing and housing, dynamic force of the cam shaft assembly and rocker shaft assembly, and bolting torque were applied as the loading conditions. The fixed points of the stud bolt were restrained and the lower support face was also restrained.

4. Result and Consideration

The stiffness of the valve train parts consists of of those of the cam shaft, cross-head, rocker shaft, bracket, and rocker arm, in order of contribution. The contribution percentage can be estimated using Eq. (6) to Eq. (10); for the intake side, the rocker arm is 33.5%, the rocker shaft and bracket are 30.3%, the cam shaft is 15.4%, cross-head is 20.6%; for the exhaust side, the rocker arm is 24.4%, the rocker shaft and bracket are 32.1%, the cam shaft is 13.1%, and the cross-head is 30.2%. Figures 7, 8, and 9 represent the tappet lift, velocity, and acceleration, respectively, for the cases of $12000N/mm$ and $20898N/mm$ overall stiffness. The influence of the stiffness on tappet lift and velocity is not significant. But the tappet acceleration is changed by about $214mm/\text{sec}^2$ at the maximum value, and the constant acceleration period gets longer during the deceleration section. The high acceleration can cause breaking of the cam contact surface, so the extremely high acceleration section should be reduced and the deceleration curve should be smooth. Within the given conditions, the wide maximum acceleration period is better for heavy-duty high speed diesel engine, but its limit is determined by the cam radius and natural frequency of the valve train. The maximum acceleration period is determined by the rotational speed of the cam, and the maximum value of acceleration is determined by the cam radius. The numerous experimental data on the acceleration period and natural frequency provides good results.

In Fig. 10 the ramp section has constant velocity period over the cam angle range $57° \sim 68°$, and after that the constant acceleration period follows over the cam angle range $68° \sim 78°$. The ramp section can be determined as 75% of the ramp end lift to total ramp lift. The ramp lift during the constant velocity period, that is, ramp rate is related with the seating velocity of valve; therefore a small ramp rate can reduce noise and stress of the valve in the seating state. In the case that the cam section, which is from 37.5° to 55° when

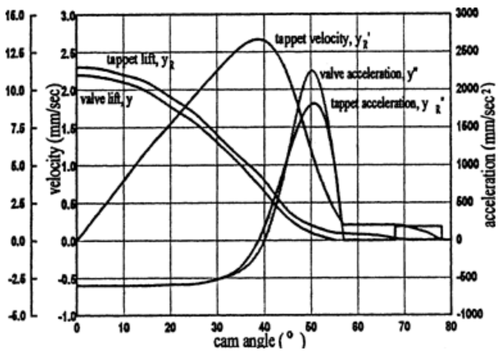

Fig. 10 Lift, velocity and acceleration curve

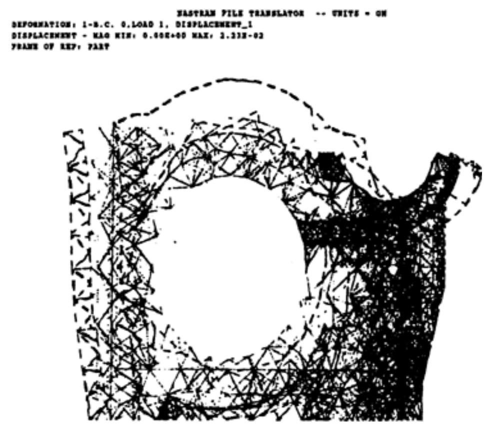

Fig. 11 Deformation of cap and support bracket

the overall stiffness is $12000N/mm$, is getting longer, the breathing volumetric efficiency of the high speed engine can be increased. The changeable valve lash under operation of the valve train and steep slope of the valve lash is advantageous for valve timing, but it can increase the seating velocity of the valve. Therefore the optimal value between these conditions should be selected.

The deformation of the bracket consisting of the cap and support is represented in Fig. 11. The radial directional deformation due to the camshaft is higher than the deformation due to the bolt.

5. Conclusion

The effect of stiffness on valve train behavior was investigated for OHC type valve trains. The stiffness contribution of the valve train parts was analyzed, and valve lift, velocity, and acceleration change were investigated according to the change in stiffness of the cam shaft bracket. The summary of the obtained results are as follows:

(1) As the stiffness increases, the maximum value of the valve acceleration increases by about $214m/\sec^2$, and the constant acceleration section has a slight tendency to increase during the deceleration period. It can be fixed by decreasing the maximum acceleration value and by adding a smooth deceleration period through stiffness change of the materials. As the stiffness increases, the cam angle period of the acceleration sine curve increases by about 1.5°, and it is disadvantageous for high speed engines.

(2) The ramp section can be determined to be about 75% of the ramp end lift to total ramp lift. The ramp lift in constant velocity period, that is ramp rate is related with seating velocity of valve, therefore small ramp rate can reduce noise and stress of valve in seating state.

(3) It was determined that material change of valve train parts can change the dynamic behavior of the valve and cause deformation. The cam form considering stiffness effects makes allowances for the static and dynamic deflections of the valve train at the cam design speed. For more accurate prediction of valve behavior, data on the applied force, position, and torsional vibration characteristics is needed through the finite element method and experiments.

References

Barkan, P., 1953, "Calculation of High-Speed Valve Motion with a Flexible Ovehead Linkage," *SAE National Passenger-Car, Body, and Materials Meeting*, Detroit, March, pp. 687～700.

Chan, C. and Pisano, A. P., 1987, "Dynamic Model of a Fluctuating Rocker-Arm Ratio Cam Systems," *Transactions of ASME*, Vol. 109, September, pp. 356～365.

Chen, F. Y., 1973, "Kinematic Synthesis of Cam Profiles for Prescribed Acceleration by a Finite Integration Method," *Journal of Engineering for Industry*, May, pp. 519～524.

Dudley, W. M., 1948, "New Methods in Valve Cam Design," *SAE Quartely Transactions*, Vol. 2, No. 1, January, pp. 19～33.

Hrones, J. A., 1948, "An Analysis of the Dynamic Forces in a Cam-Driven System," *The American Society of Mechanical Engineers*, July, pp. 473～482.

Kim, W. J., Jeon, H. S., and Park, Y. S., 1990, "Analytical and Experimental Motion Analysis of Finger Follower Type Cam-Valve System with a Hydraulic Tappet," *KSME Journal*, Vol. 4, No. 1, pp 40～47.

Kwakernaak, H. and Smit, J, 1968, "Minimum Vibration Cam Profiles," *Journal Mechanical Engineering Science*, Vol. 10, No. 3, pp 219～227.

Mattew, G. K. and Tesar, D., 1978, "The Design of Modeled Cam Systems (Minimization of Motion Distortion Due to Modelling Errors)," *Journal of Engineering for Industry*, November, pp. 1181～1189.

Mercer, S. and Holowenko, A. R., 1958, "Dynamic Characteristics of Cam Forms Calculated by the Digital Computer," *Transaction of ASME*, November, pp. 1695～1705.

Roggenbuck, R. A., 1953, "Designing the Cam Profile for Low Vibration at High Speeds," *SAE National Passenger-Car, Body, and Materials Meeting*, Detroit, March, pp. 701～705.

Sakai, H. and Kosaki, H., 1976, "Analysis of Valve Motion in Overhead Valve Linkage-Roles of Valve Spring Surge in Valve Motion-," *Journal of the Faculty of Engineering*, May, pp. 441～446.

Seidlitz, S., 1990, "An Optimization Approach to Valve Train Design," *SAE* 901638, pp. 1～11.

Shooter, S. B., West, R. B. and Reinholtz, C. F., 1994, "An Unified Approach to Teaching Analytical Cam Design Using Conjugate Geometry," *International Journal of Mechanical Engineering Education*, Vol. 23, No. 2, June, pp. 145～156.

Yan, H., Tsai, M. and Hsu, M., 1996, "A Variable-Speed Method for Improving Motion Characteristics of Cam-Follower Systems," *Transactions of ASME*, Vol. 118, June, pp. 250～258.